Appl. Phys. B
DOI 10.1007/s00340-014-5883-1

Applied Physics B
Lasers and Optics

Line intensity measurements of methane's v_3-band using a cw-OPO

Marco P. Moreno · Malo Cadoret · Mohammad Jahjah · Linh Nguyen · Flavio C. Cruz · Jean-Jacques Zondy

Received: 18 April 2014 / Accepted: 10 June 2014

Abstract We report on absolute line strength measurements of P(1), R(0) and R(1) singlet lines in the 3.3 μm v_3 (C–H stretching) band of methane $^{12}CH_4$ at reference temperature $T = 296$ K. Line strength measurements are performed at low pressure ($P \leq 1$ Torr) using direct absorption spectroscopy technique based on a widely tunable continuous-wave singly resonant optical parametric oscillator. The 1σ overall accuracy in line strength determinations ranges between 7 and 8 % mostly limited by pressure and frequency measurements. A comparison with previous reported values is made. Our results show good agreement with the HITRAN 2012 database.

1 Introduction

The mid-infrared (MIR) spectral region (3–30 μm) is a domain of interest to many areas of science and technology. Most fundamental rovibrational transitions of simple molecules fall in this region of the electromagnetic spectrum making it ideal for spectroscopic detection. In this context, absolute line intensity measurements of molecular spectral lines in the MIR finds a variety of applications in different research fields such as molecular astrophysics [1], global environmental monitoring [2], atmospheric chemistry, homeland security, trace gas sensing and medical diagnostics among others. Indeed, accurate knowledge of a spectroscopic parameter such as line strength, which characterize the ability of a molecule to absorb radiation, is indispensable when one wants to retrieve the gas concentration in the troposphere or the lower stratosphere [3] with high accuracy [4]. Moreover, theoretical simulations of climate change or planetary atmospheres need accurate spectroscopic parameters input such as line strengths to improve the accuracy of their modeling.

Even though large amounts of spectroscopic parameters can be found in databases such as HITRAN [5] which combine experimental measurements with theoritical calculations, there exist an actual need for novel accurate and traceable measurements in this spectral domain for a variety of simple molecules such as methane which is known to be a greenhouse gas of major importance in the radiative balance of the Earth's climate [6].

Absorption spectroscopy for line strength measurements of methane in the v_3 band has been performed in the last decades using low resolution instruments such as grating spectrometers [7] or FTIR spectrometers [8]. The first measurements using tunable narrow linewidth ($\Delta v \approx 5$ MHz) mid-IR laser was performed by Pine who employed nonlinear difference-frequency generation (DFG) of two tunable dye lasers in $LiNbO_3$ to generate microwatt level of 3.3–3.4 μm coherent radiation [9–11]. More recently, in-situ atmospheric DFG laser spectroscopy of the v_3 band of CH_4 (3.25–3.25 μm) using a compact periodically-poled lithium niobate-based setup with sub-10-MHz resolution has been reported for in-situ spectroscopy of methane in the troposphere and lower stratosphere regions [2].

M. P. Moreno · M. Cadoret (✉) · M. Jahjah · L. Nguyen · J.-J. Zondy
Laboratoire Commun de Métrologie LNE-Cnam, 61 rue du Landy, 93210 La Plaine Saint Denis, France
e-mail: malo.cadoret@cnam.fr

M. P. Moreno
Departamento de Física, Universidade Federal de Rondônia, Campus Ji-Paraná, Rondônia 76900-726, Brazil

F. C. Cruz
Instituto de Física Gleb Wataghin, Universidade Estadual de Campinas, Campinas, SP 13083-859, Brazil

Published online: 20 June 2014

In this paper, we report on line strength measurements of the P(1), R(0) and R(1) transitions in the v_3 band of CH_4 by direct absorption spectroscopy (DAS) using a tunable continuous-wave optical parametric oscillator (cw-OPO). Widely tunable (2.8–4.3 μm) singly resonant PPLN-OPOs (SROs) pumped by amplified Yb-fiber output at 1,064 nm are powerful (Watt level) candidates as tunable narrow linewidth ($\Delta v <$ 100 kHz) MIR sources to perform high-resolution spectroscopy in the 3–3.4 μm range for line parameter investigation [12, 13], with respect to low-power (μW-level) DFG lasers with limited tunability [14, 15]. A single-grating PPLN-SRO can conveniently cover the entire v_3 band of methane, especially if the pump laser is mode-hop-free tunable over tens of nanometers around 1,064 nm [16]. The only inconvenience of cw SROs against DFG lasers is the tendency of parametric oscillators' signal wave to mode-hop during the pump scan, due to the intrinsic low cw parametric gain which scales as the round-trip signal cavity loss. This mode-hopping behavior can be long-term frozen by active stabilization of the signal resonator length [17]. However, for line-by-line spectroscopy which require only moderate pump tuning over $<$10 GHz, active stabilization is superfluous as in the present work provided that the scan rate is much faster than the average time between two successive mode-hop events. To retrieve the line strength S_{if} of a rovibrational transition between initial energy level E_i and final level E_f [18], we use a basic approach based on the classical Beer Lambert's absorption law for which we measure the integrated absorbance for a known temperature, pressure and path length. Our results are compared to previous reports including HITRAN 2012 database [5].

2 Description of the laser spectrometer

2.1 The singly resonant OPO spectrometer

The spectrometer is a continuous-wave, single frequency optical parametric oscillator (cw-OPO) based on a 5 %-Magnesium oxide-doped periodically-poled congruent lithium niobate (ppMgCLN) nonlinear crystal [16, 17]. It is implemented as a pump-wave-tuned singly resonant oscillator (SRO), for which only the signal wave arising from the pump photon down-conversion process ($v_p = v_s + v_i$) is resonated inside a bow-tie ring cavity. The singly resonant configuration allows convenient continuous tuning of the idler beam frequency (v_i) simply by tuning the pump frequency (v_p). The full pump excursion is transferred to the idler, by virtue of the fixed frequency of the signal wave, kept in resonance with the cavity [17]. The maximum achievable mid-IR continuous tuning range is hence only determined by the pump-tuning-induced phase-mismatch $\Delta k = k_p - k_s - k_i - 2\pi/\Lambda$ (where Λ is the ppMgCLN grating period growth and $k_{p,s,i}$ are the wave-vectors) which controls the OPO parametric gain $\propto \mathrm{sinc}^2(\Delta \mathrm{kL}/2)$ where L is the crystal's length. For an idler wave emission near 3.3 μm, the change in Δk induced by the pump scan over several nanometers is extremely small (quasi non-critical phase-matching [16]), resulting hence in a wide continuous Δv_i excursion before a mode-hop event occurs following the gain decrease.

The OPO is pumped by an elaborate commercial single frequency master external cavity diode laser (ECDL, New Focus Velocity™ Widely Tunable Laser, model 6321). This ECDL is mode-hop-free (MHF) tunable between 1,050 and 1,070 nm, with a narrow linewidth [16](300 kHz at 1 ms), and amplified by a 10 W polarization-maintaining Yb:fiber amplifier. The oscillating signal wave inside the OPO cavity is comprised between 1,450 and 1,650 nm (set by the high reflectivity mirrors coating bandwidths), leading to a down-converted idler wave in the MIR tunable between 3 and 4 μm when the nonlinear crystal temperature and (or) the pump wavelength are (is) changed. Moreover, in order to reduce mode-hop events, a YAG etalon with a thickness of 400 μm was placed between the two plane mirrors of the OPO cavity. For continuous tuning range over several nanometers [16], the DC-motor attached to the ECDL end-mirror can apply fast rotation tilt (at a speed $<$20 nm/s) of the end-mirror of the Littman-Metcalf type external cavity design.

Since full widths of molecular transitions do not exceed 3 GHz at atmospheric pressures, for the spectroscopy of the R(0), R(1) and P(1) lines, only moderate idler tuning over $<$10 GHz is required. This is performed by a voltage ramp applied to the piezoelectric transducer (PZT) attached to the feedback mirror of the ECDL. The PZT maximum tuning range of 50 GHz eliminates the need of other long range tuning methods, such as using DC-motor.

The major advantage of our SRO spectrometer is the use of a widely MHF tunable ECDL (instead of a Yb:fiber laser which can be tuned over $\sim$ 1 nm only). The large MHF tuning capability of the ECDL combined with the temperature tuning of the ppMgCLN nonlinear crystal extends the phase-matching capability of the OPO [16]. As an example, to target the singlet lines under investigation only the grating period $\Lambda = 30.5$ μm is used with a phase-matched combination (λ_p, T) where the regulated grating temperature $T(\Delta T = \pm 0.1^o\mathrm{C})$ is varied between 90°C and 105°C and the ECDL pump wavelength is set between 1,063 and 1,064 nm. For instance, the R(0) and R(1) lines spaced by $\sim$10 cm^{-1} can be accessed by decreasing the pump laser wavelength from 1,064 nm-R(1)- to 1,063 nm-R(0)- at constant temperature $T = 102$°C of ppMgCLN.

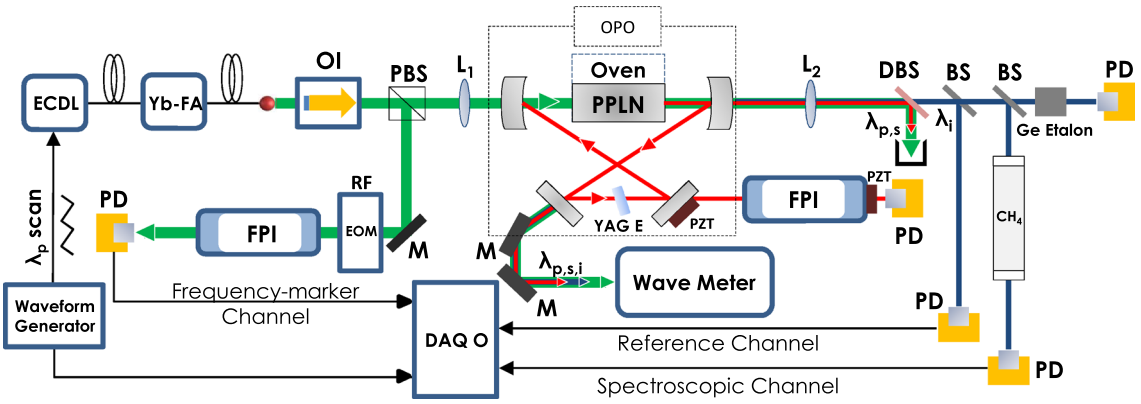

Fig. 1 Spectrometer based on singly resonant OPO for the spectroscopy of the ν_3 band of methane in the 3.3 μm range. The idler output is divided into a spectroscopic channel (containing the cell) and a reference channel monitoring the idler baseline. A frequency-difference marker in the idler range, provided by the two ± 30 MHz sidebands of the RF phase-modulated pump, allows to accurately calibrate the time (frequency) axis of the recording oscilloscope. For the detailed description of the OPO source setup, see Refs. [16, 17]. *ECDL* extended-cavity diode laser, *M* mirror, *BS* beam splitter, *PBS* polarization beam splitter, *L* lens, *DBS* dichroic beam splitter, *YAG E* YAG etalon, *PD* photodetector, *EOM* electro-optic modulator, *FPI* Fabry-Pérot interferometer, *PZT* Piezoelectric transducer, *Yb:FA* Yb-fiber amplifier, *OI* optical isolator

Compared to a fixed λ_p pump laser for which only temperature tuning controls the phase-matching, keeping the chip temperature unchanged in our case further enforces the stability of the resonator pathlength. Although the P(1) line, spaced by -20cm^{-1} from the R(0) line, could be accessed in a similar way by setting the pump to 1,067 nm, in this case, the Yb:fiber amplifier gain bandwidth is reduced. To by-pass this inconvenience, we have stepped-down the ppMgCLN temperature to T = 90°C for which the phase-matching (PM) condition ($\Delta k = 0$) is satisfied at the P(1) transition for a pump near 1,064.2 nm.

2.2 Experimental setup for direct absorption spectroscopy (DAS)

The experimental setup used to perform direct absorption spectroscopy of R(0), R(1) and P(1) singlet lines of methanes ν_3 band is sketched on Fig. 1. A 10-cm-long absorption cell, equipped with BaF_2 tilted windows, contains low pressure ($P \lesssim 1$ Torr) of pure CH_4 in natural abundance (^{12}C purity 99.99 %), and its total pressure is measured with a capacitive pressure gauge (Baratron model 626 BX01TBE, not shown). We consider that the cell temperature is the same as the temperature measured by our room temperature sensor ($T = 296$ K) in a regulated air conditioning environment.

The idler beam exiting the OPO cavity is filtered from the residual pump and signal by a dichroic beam splitter (DBS). The residual pump and signal power relative to the idler are estimated to be <0.1 % after the DBS. After filtering, a small fraction of the idler power is sent to a solid Ge etalon with a free spectral range (FSR) of 1.43 GHz at 3.3 μm. This Ge etalon is used to discard any non-single frequency scan of the OPO when addressing broadband scans over a large frequency range (>70 cm^{-1}) [16].

Most of the remaining idler power is then divided into two channels. The first channel is the "spectroscopic channel," where the idler beam is sent to the absorption cell. The transmitted power through the cell is monitored with an InAs photodetector (PD) and recorded on a digital oscilloscope (Lecroy Model Wavejet 334A, 2 GS/s) and saved for data analysis.

The second channel serves as a "reference channel." An InAs PD placed on this channel replicates any intensity fluctuations and amplitude modulation in the spectroscopic channel. In any case, care was made to minimize as well as possible the unavoidable spurious interference fringes affecting the idler power baseline, due to feedback from the PDs, but mainly to the non-perfect anti-reflective coatings of the ppMgCLN crystal in the idler band ($R > 20$ %), which leads to a weak fringing pattern with a $\sim$ 1.5 GHz of FSR corresponding to the sub-cavity formed by the crystal end facets.

A third channel, "frequency marker channel," is used to measure the frequency scan of the pump laser during the experiment. A 30 MHz-driven electro-optic phase modulator (EOM, Model 4001 New Focus) is inserted just before the (non-scanned, non-biased) pump Thorlabs Fabry-Pérot interferometer (FPI, with FSR = 1.5 GHz and finesse = 200 at 1,064 nm) so as to create two sidebands at ±30 MHz, providing thus a 60 MHz marker to calibrate in a relative way the MIR frequency scale. We remind that in a SRO, the pump frequency scan is fully transferred to the idler wave ($\Delta\nu_p = \Delta\nu_i$). In the Doppler regime corresponding to the low gas pressure used ($P < 1$ Torr) the FWHM of the lines is typically $\Delta\nu_D \approx 300$ MHz. Thus, a frequency scan

range of the order of 1.5 GHz is sufficient to capture any line.

To perform line-by-line absorption spectroscopy, the idler wave frequency is first set at a frequency close to the HITRAN documented line position, which is checked by the readout of the Michelson-type MIR wave meter (Bristol Instruments, with a 10^{-6} relative accuracy). Then a frequency generator (Rigol model DG3121A) is used to deliver an analog (voltage offset biased) triangular voltage that drives the PZT of the ECDL. This triangular ramp triggers all the three other channels of the oscilloscope to which all PD outputs are connected: the reference channel, the spectroscopic channel and the reference marker channel (which should display at least one FPI pump fringe and its two sideband markers). The centering of the spectroscopic pattern near the middle of the descending ramp can be made by either varying the offset ramp voltage in ± 10 mV steps, or by adjacent mode-hop tuning of the oscillating signal mode, which is achieved by manual change of the high voltage applied to the PZT attached to one of the OPO mirrors. When an accidental signal mode-hop occurs, the spectroscopic pattern can be conveniently retrieved by manual change of this high voltage until the initial oscillating signal mode is recovered. The incident idler power on the sample cell is typically comprised between 0.2 and 0.4 W, corresponding to an OPO driven at two times above the pump threshold ($P_{\text{th}} = 3$W).

3 Line strength measurements

3.1 Direct absorption spectroscopy

Our measurement procedure relies on accurate detection of the attenuation of the coherent idler radiation absorbed by the methane molecules. Due to the large oscillator strengths in the v_3 fundamental band, the cell transmission saturates beyond $P = 1.2$ Torr for a cell length of $L = 10$ cm, which is the reason why the gas pressure was restricted to $P < 1$ Torr. The absorption process that takes place in the sample cell is governed by the classical Beer–Lambert's law which states that the transmitted light power P with frequency $\tilde{\nu}$ (in cm^{-1}) decreases as:

$$P(\tilde{\nu}) = P_0 e^{-S(T)g(\tilde{\nu}-\tilde{\nu_0})nL}, \quad (1)$$

where P_0 is the incident light power, $\tilde{\nu_0}$ is the line center frequency, n is the gas density (in molecules·cm^{-3}), L is the absorption path length (in cm), $S(T)$ the gas temperature-dependant line strength (in cm/molecule) [18] and $g(\tilde{\nu} - \tilde{\nu_0})$ is the normalized absorption lineshape that we will consider to be a Voigt profile which takes into account both Doppler and collisional broadening mechanisms. From Eq. 1, one can derive the integrated absorbance of the line which is obtained from our recorded spectra:

$$A_{\text{line}} = \int \ln\left[\frac{P_0}{P(\tilde{\nu})}\right] d\tilde{\nu} = S(T)Ln \quad (2)$$

Considering an ideal gas ($P = nk_BT$), one can determine the gas density n from the measurements of pressure P and temperature T.

Hence, if the length L of the cell is known, one obtains the strength of the line from Eq. 2:

$$S(T) = \frac{k_BT}{PL} A_{\text{line}} \quad (3)$$

where $k_B = 1.38065 \times 10^{-23}$ J/K is the Boltzmann constant. Hence, plotting A_{line} as a function of the reduced pressure parameter $x = PL/k_BT$ yields the line strength S as the slope of the fitted straight line over x.

3.2 Measurements and data analysis

To avoid any interfering lines and to avoid line mixing effects, we chose the three singlet lines of the v_3 band of CH_4: P(1), R(0) and R(1) at 3,009.011267 cm^{-1}, 3,028.752175 cm^{-1} and 3,038.498427 cm^{-1}, respectively. The absorption profile for a given rovibrational transition is recorded as a function of the total CH_4 pressure in the cell which is varied between 0.1 and 1.1 Torr. The absorbance spectra are fitted with an iterative nonlinear least-squares procedure assuming a Voigt lineshape for the normalized g function. The integrated absorbance A_{line} of the line is retrieved from the fit algorithm of the experimental data.

Depending on the CH_4 pressure in the cell, extra-care must be taken to the frequency scanning range δ around the absorption peak (i.e., the beginning and end point around the absorption peak has to be carefully selected). Indeed, a limited integration interval can lead to an uncertainty in the measured line strength because part of the wings of the line profile are neglected. To study this effect, we have simulated in Fig. 2a the normalized Voigt profile and its integrated area as a function of frequency in the case where the CH_4 pressure in the cell is $P = 1.1$ Torr (our maximum pressure used in the experiment) and temperature $T = 296$ K. For this simulation, the Lorentzian width due to collisional broadening is $\gamma_L = 0.2$ MHz and the Doppler width associated with random thermal motion of the absorbing molecules is $\gamma_D = 280$ MHz assuming a Maxwellian velocity distribution. As we can see, we have a gaussian-like profile that rapidly drops because $\gamma_L \ll \gamma_D$. The error associated with the total scanning range $\delta = N\times$FWHM (expressed in integer number N, of the full width half maximum of the absorption line), is shown in Fig. 2b. The reference is set to be at 20×FWHM and for our

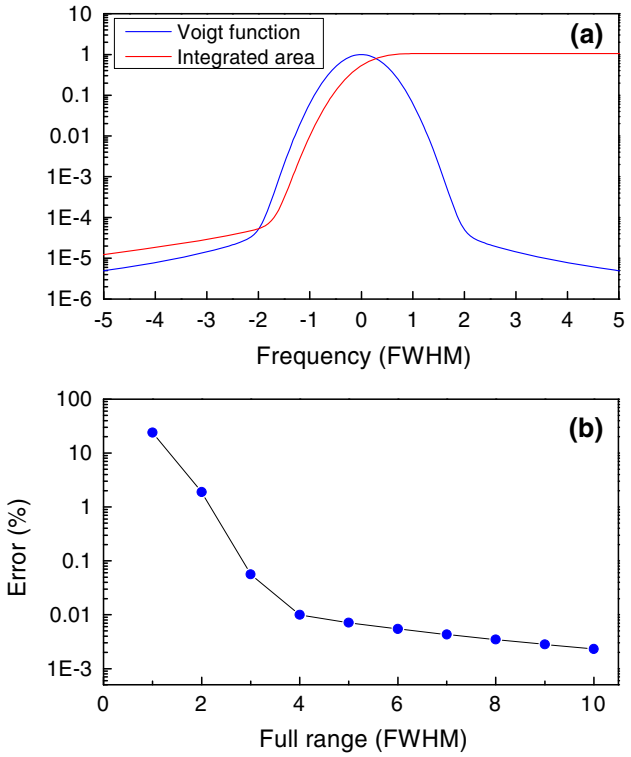

Fig. 2 **a** Voigt profile normalized (*blue curve*) as a function of frequency (in cm^{-1}), in units of FWHM. The *red curve* is the integrated area considering a Voigt lineshape. **b** Error in the calculated area as a function of the total scanning range for pressure $P = 1.1$ Torr and temperature $T = 296$ K

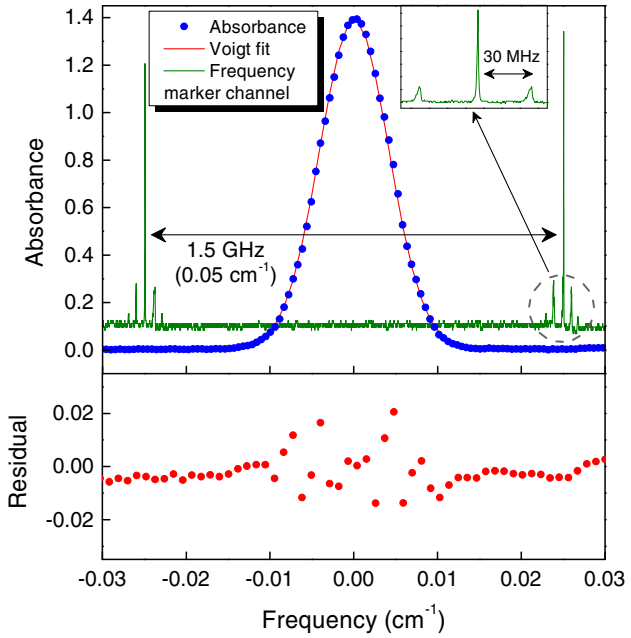

Fig. 3 *Top*: typical absorbance curve ($\ln[P_0/P(\tilde{\nu})]$, *blue dots*), and its best fit (*red curve*) for the R(1) line at pressure $P = 0.51$ Torr, $S/N = 150$. The *green curve* is the transmission of the FPI (vertically shifted for better clarity) which allows to frequency-calibrate the *horizontal scale*. *Bottom*: residual of the fit

measurements, we have considered a scanning range of at least $\delta = 5\times$FWHM, which ensures an error on the integrated area below 0.01 %.

Calibration of the frequency scale is performed by means of phase modulation sidebands (±30 MHz originating from a waveform function generator) of the pump carrier generated by an electro-optic modulator (EOM) (Fig. 1). We have calibrated carefully the FSR of the pump confocal FPI using these markers, and under various scan speeds to estimate the possible nonlinearity of the pump laser PZT. At slow scan rate (1–3 Hz), the PZT nonlinearity is minimized. From a statistical calibration of the FSR using the two side-band markers, we found a FSR value of 1,500 (±1 %) MHz. These frequency markers are used for each measurement, hence minimizing errors due to hysteresis and nonlinearities (depending on the scanning speed) of the PZT during the pump frequency tuning.

An example of R(1) line absorption spectrum at pressure $P = 0.51$ Torr is reported on Fig. 3 (blue dot) where the number of digitized points is reduced to 100 and the observed signal-to-noise ratio is $S/N = 150$. The best fit curve is also shown (red curve) considering a Voigt lineshape. Transmission of the pump FPI (vertically shifted for clarity sake) allowing to frequency-calibrate the horizontal scale is also shown (green curve). The fit residual shows slight asymmetry in the absorbance wings that may originate from residual fringing modulations on the idler baseline.

4 Uncertainty analysis and results

Line strengths of R(0), R(1) and P(1) lines are inferred from Eq. 3 with a typical statistical uncertainty of 0.3 % originating from the fitting procedure. On Fig. 4, we show the histogram of 69 independent determinations of R(1) line strength calculated from Eq. 3, for a pressure range between 0.09 and 0.88 Torr. Dispersion in the results due to measurement repeatability presents a relative standard deviation (1σ) of 5.6 %. Thus, statistical uncertainty of the fit procedure is not the limiting factor.

Dispersion in the results originates from both uncertainties on the frequency-scale calibration (affecting the A_{line} value) and on the $x = PL/k_BT$ parameter. In order to account for these biases, we estimated uncertainties on both variables. The uncertainty in the frequency-scale calibration is at least 1 % of the FSR of the FPI (5×10^{-4} $cm^{-1} = 15$ MHz). On the other hand, we estimate uncertainties on pressure P, length L and temperature T to be 5, 1 % and 0.2 K, respectively. Relative uncertainty

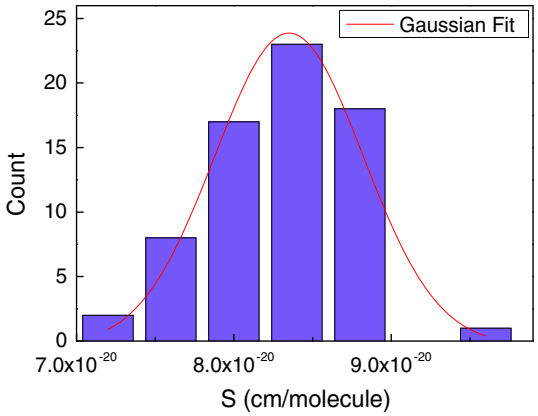

Fig. 4 Distribution of the R(1) line strength determinations for 69 measurements, calculated from Eq. 3, with a pressure P ranging from 0.09 to 0.88 Torr. The expected value obtained from the Gaussian fit (*red curve*) is 8.35×10^{-20} cm/molecule, with a standard deviation of 4.7×10^{-21} cm/molecule

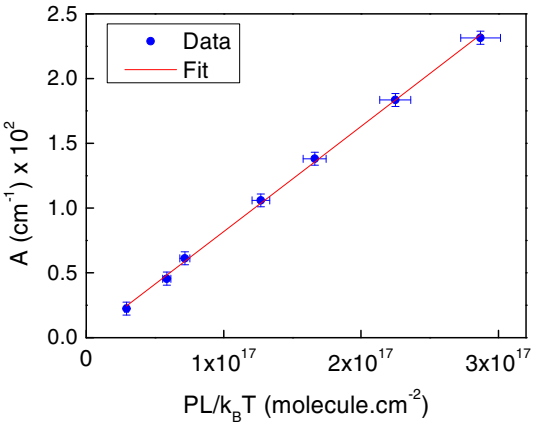

Fig. 5 Integrated absorbance of the R(1) line as a function of PL/k_BT. In this curve, the pressure is varying between 0.23 and 1.1 Torr, and each data point is an average of 10 recordings. The line strength S is determined by the slope of the linear fit

on the pressure is not the specified uncertainty of the pressure gauge readout (0.5 %). This 5 % uncertainty takes into account our vacuum system tubing specificity, as well as the elapsed spectroscopic measurement time after the cell has been filled (the Swagelok fittings and valve displays a slow leak).

Other sources of errors may also affect the measured line profile, such as saturation effects or nonlinearity of the photodetector when using high laser power source especially in the mid-IR. Nevertheless, in our experiment, the estimated saturation parameter ($s \ll 1$) ensures linear absorption conditions as well as neglectable power broadening. Moreover, we did not see any nonlinear response of our detector with respect to any incident idler power (the transmitted power is attenuated down to sub-mW level with a neutral density filter, which is well within the linearity zone of the detector).

The final value of the line strength for each line was finally determined from the slope of a weighted linear fit taking into account the errors on both x and A_{line}.

Figure 5 shows the integrated absorbance A_{line} as a function of $x = PL/k_BT$ for the R(1) line. Each point is obtained from the mean value of approximately 10 recorded spectra and an error bar on each variable is added.

From the slope of the weighted linear fit (red curve), we infer the line strength $S = 8.25(38) \times 10^{-20}$ cm/molecule. The intercept of the linear fit with the vertical axis is $(-0.8 \pm 4.4) \times 10^{-4}$ cm^{-1}, which is compatible with the assumption that $A_{\text{line}}(x = 0) = 0$, meaning that the biases that may induce systematic shifts have been well taken into account. This result is in agreement with HITRAN 2012 database [5] for R(1) line: $S = 8.85(66) \times 10^{-20}$ cm/molecule, although our value is -7 % lower.

Previous measurements of the R(1) line strength using a difference-frequency (DFG) spectrometer have been reported in the literature. Dang-Nhu et al obtained $S = 8.994 \times 10^{-20}$ cm/molecule in 1979 [11], -1 % away from a theoretical value they calculated. However, the uncertainty in the individual line-by-line strengths is not given. Twenty years later, Pine's re-measurement of this line strength using a DFG spectrometer based on the difference-frequency of two dye lasers with a $\sim$5 MHz resolution yielded $S = 8.911(34) \times 10^{-20}$ cm/molecule [10]. Our value agrees, within the uncertainty bars, with all these measurements.

We measured line strengths of P(1) and R(0) lines following the same procedure as above. The line strength determinations of P(1), R(0) and R(1) lines are listed in Table 1 and compared to previous work performed by Pine et al, Dang-Nhu et al as well as to the HITRAN 2012 database (the line strength of P(1) was not in the list published by Dang-Nhu et al).

From Table 1, we infer an overall relative uncertainty on the measured line strengths of 7.7 %, comparable with the HITRAN 2012 uncertainties (7–8 %).

5 Conclusions

In this paper, we have presented the results of P(1), R(1) and R(0) line strengths determinations at 3 microns by use of a continuous-wave singly resonant OPO spectrometer associated with direct absorption spectroscopy method. This work is to our knowledge the first CH_4 line intensity determination by use of a cw-OPO spectrometer (though a first line strength measurement of a CH_3I rovibrational line at 3.4 μm using a similar OPO spectrometer has been

Table 1 Line strength, S, in units of 10^{-20} cm/molecule

$\Delta J(J'')$	$C' \leftarrow C''$	$n(v'_n \leftarrow v''_n)$	Frequency (cm^{-1})	Ref. [10]	Ref. [11]	HITRAN 2012	This work
P(1)	F2 ← F1	3(1 ← 0)	3,009.011406	1.669 (31)	–	1.71 (13)	1.62 (23)
R(0)	A2 ← A1	3(1 ← 0)	3,028.752260	9.181 (41)	9.292	9.21 (69)	9.05 (40)
R(1)	F2 ← F1	3(1 ← 0)	3,038.498494	8.911 (34)	8.994	8.85 (66)	8.25 (38)

C is the rovibrational symmetry, v_n is the quantum number associated with the vibrational mode n, and J is the total angular momentum excluding nuclear spin. The upper and lower states are referenced by the $'$ and $''$ symbols, respectively

reported in [12]). The overall relative uncertainty on the line intensity parameters are comparable to HITRAN 2012 database and mostly limited by the frequency-scale relative uncertainty on the experimental lineshape-fitted data, the presence of residual idler fringes on the baseline and the slight nonlinearity of the pump frequency scan. Because we have addressed singlet components, line mixing effects are quite negligible, as well as small possible interference with weak lines of other absorbing species owing to the DAS method. In order to improve our accuracy, shot-to-shot amplitude fluctuation of the idler power and residual etaloning effects should be canceled via an intensity stabilization of the idler beam. Finally, to drastically reduce the frequency axis calibration uncertainty, an Er:fiber femtosecond optical frequency comb-assisted DAS, that monitors the absolute frequencies of the scan [12, 14], should enable us to avoid the problem of the PZT nonlinearity.

Acknowledgments The authors acknowledge partial support from a FP7- EURAMET grant (contract No ENV-06). M. P. Moreno thanks CAPES for postdoctoral fellowship support under BEX-12610-12-7. The authors thank PHC-Capes Cofecub program (project code: 25060RE) for support.

References

1. C.R. Webster, Appl. Opt. **44**, 1226–1234 (2005)
2. M. Ghysels, L. Gomez, J. Cousin, N. Amarouche, H. Jost, G. Durry, Appl. Phys. B **104**, 989–1000 (2011)
3. E.C. Richard, K.K. Kelly, R.H. Winkler, R. Wilson, T.L. Thompson, R.J. Mclaughlin, A.L. Schmeltekopf, A.F. Tuck, Appl. Phys. B **75**, 183–194 (2002)
4. P. Malara, P. Maddaloni, G. Gagliardi, P. De Natale, Opt. Express **14**, 1304–1313 (2006)
5. L.S. Rothman et al., J. Quant. Spectrosc. Radiat. Transf. **130**, 4–60 (2013)
6. P. Forster, V. Ramaswamy, P. Artaxo, T. Berntsen, R. Betts, D.W. Fahey, J. Haywood, J. Lean, D.C. Lowe, G. Myhre, J. Nganga, R. Prinn, G. Raga, M. Schulz, R. Van Dorland. in *Climate Change 2007: The Physical Science Basis. Contribution of Working Group I to the Fourth Assessment Report of the Intergovernmental Panel on Climate Change*, ed. by S. Solomon, D. Qin, M. Manning, Z. Chen, M. Marquis, K.B. Averyt, M. Tignor, H.L. Miller (Cambridge University Press, Cambridge, 2007)
7. P. Varanasi, S. Sarangi, L. Gugh, Astrophys. J. **179**, 977–982 (1973)
8. R.A. Toth, L.R. Brown, L.H. Hunt, L.S. Rothman, Appl. Opt. **20**, 932–935 (1981)
9. A.S. Pine, J. Opt. Soc. Am **66**, 97–108 (1976)
10. A.S. Pine, J. Quant. Spectrosc. Radiat. Transf. **57**, 157–176 (1997)
11. M. Dang-Nhu, A.S. Pine, A.G. Robiette, J. Mol. Spetrosc. **77**, 57–68 (1979)
12. I. Ricciardi, E. Tommasi, P. Maddaloni, S. Mosca, A. Rocco, J.-J. Zondy, M. De Rosa, P. De Natale, Mol. Phys. **110**, 2103–2109 (2012)
13. I. Ricciardi, E. Tommasi, P. Maddaloni, S. Mosca, A. Rocco, J.-J. Zondy, M. De Rosa, P. De Natale, Opt. Express **20**, 9178–9186 (2012)
14. S. Okubo, H. Nakayama, K. Iwakuni, H. Inaba, H. Sasada, Opt. Express **19**, 23880 (2011)
15. M. Abe, K. Iwakuni, S. Okubo, H. Sasada, J. Opt. Soc. Am. B **30**, 1027–1035 (2013)
16. J. Courtois, R. Bouchendira, M. Cadoret, I. Ricciardi, S. Mosca, M. De Rosa, P. De Natale, J.-J. Zondy, Opt. Lett. **38**, 1972–1974 (2013)
17. Andrieux Emeline, Zanon Thomas, Cadoret Malo, Rihan Abdallah, Zondy Jean-Jacques, Opt. Lett. **36**, 1212–1214 (2011)
18. K. Fox, Phys. Rev. A **8**, 658–662 (1973)